Quality Analysis of 3D Reconstruction in Underwater Photogrammetry by Bootstrapping Design of Experiments

M. Martorelli, A. Lepore, A. Lanzotti

***Abstract*—**Nowadays photogrammetric techniques have known important developments and are widely employed for 3D acquisitions in different fields of application. The paper analyzes the effects of different parameters (texturization, ambient light and water turbidity) on the quality of the 3D reconstruction in underwater photogrammetry. Several experimental tests were performed on a wind turbine blade using a common action camera, the GoPro 4 black edition and a commercial software, Photoscan by ©Agisoft. By means of a DoE (Design of Experiments) approach, 3D models were reconstructed varying the chosen parameters. Each of them was compared with a CAD model, used as reference, obtained by more accurate laser scans VI-9i by Konica Minolta. The results showed that blade texturization, ambient light and water turbidity significantly impact on the quality of the 3D reconstruction. Optimal results were obtained with textured blade, morning ambient light (exposure 1/60, f/2.8 and ISO sensitivity 100) and clear water. Moreover, in order to calculate confidence intervals for regression coefficients, even with few acquisitions, a computer-intensive bootstrap procedure was applied to the regression model. Finally, further confirmation experiments carried out in a deeper swimming pool and with poor conditions (e.g., very low ambient light and no blade texturization) in order to reproduce the real submarine environment. In such situations, an additional source of light and one or more grids, which allow a pattern to be created on the edges of the wind turbine blade, may help reconstructions.

***Keywords*—** Underwater photogrammetry, Reverse Engineering, Passive No-contact Techniques, Structure From Motion, Design of Experiments, Bootstrapping.

M. Martorelli, Scientific Responsible of Fraunhofer JL IDEAS-CREAMI, is with Department of Industrial Engineering, University of Naples Federico II P.le Tecchio, 80, 80125 Naples, Italy (corresponding author. Phone/Fax: +39817682470; e-mail: massimo.martorelli@unina.it).

A. Lepore is with the Industrial Engineering Department, University of Naples Federico II, Italy (e-mail: antonio.lepore@unina.it).

A. Lanzotti, Director of Fraunhofer JL IDEAS, is with the Industrial Engineering Department, University of Naples Federico II, Italy (e-mail: antonio.lanzotti@unina.it).

I. Introduction

Nowadays Reverse Engineering (RE) techniques allows for digital 3D reconstruction of objects, even of complex shape, using principles codified in complete sets of procedures, specific to different fields of application.

In particular non-contact active and passive systems are today widely used in several industrial applications. Even if the best results have been reached using active techniques (e.g. in quality control measurements) [1], passive techniques allow us, through simple and low-cost hardware and software, to get fast and accurate 3D acquisitions. Among passive techniques, the photogrammetry has known an important development during the last decade [2] due mainly to the increase of the quality of low-cost digital cameras and the significant development of photogrammetric software [3, 4].

Photogrammetric methods are as old as photography and can be dated to the Mid-nineteenth century.

The French officer Aimé Laussedat is considered the "Father of Photogrammetry". He developed in 1849 the first photogrammetric devices and methods, using terrestrial photographs for topographic map compilation. The process was called iconometry from the Greek words icon and metry, which mean image and measurement, respectively [5].

Digital Photogrammetry instead was born in the 80's, having as a great innovation the use of digital images as a primary data source.

Digital photogrammetry is characterized by the following main phases:

- analysis of the shape of the object and planning of the photos to be taken;
- calibration of the camera;
- processing the photos with specific software to generate a point cloud;
- transfer the point cloud to CAD software to create a 3D CAD model.

The extraction of 3D information from digital images is a complex task requiring a mathematical formulation between the images, at least two, and the object. It uses methods from many disciplines, including optics and projective geometry. In particular, the fundamental principle is that of triangulation.

Due to the fact that the 3D reconstruction is performed

through the identification of common natural features in the image set, the accuracy of the reconstruction depends on the quality of images and textures. Algorithms for photogrammetry typically express the problem as that of minimizing the sum of the squares of a set of errors, known as bundle adjustment [6].

Structure from Motion (SfM) algorithms [7] is able to find a set of 3D points P, a rotation R and position t of the cameras, given a set of images of a static scene with 2D points in correspondence, as shown in Fig. 1 by color-coded points.

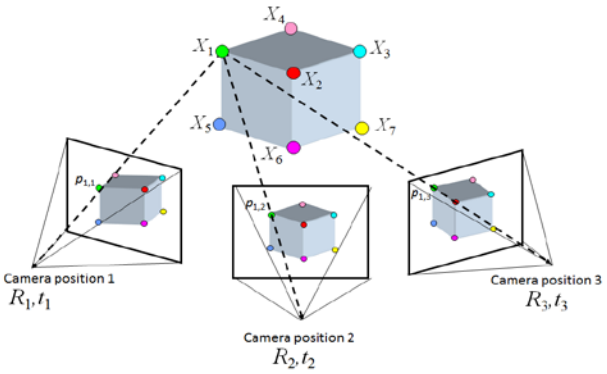

Fig. 1 Structure from Motion algorithm

This problem can be formulated as an optimization problem where rotations R, positions T, and 3D point locations P that minimize sum of squared reprojection errors (equation 1) have to be found by minimizing the following function

$$g(\mathbf{X},\mathbf{R},\mathbf{T}) = \sum_{i=1}^{m}\sum_{j=1}^{n} \underbrace{w_{ij}}_{\substack{\text{indicator variable:}\\ \text{is point } i \text{ visible in image } j \text{ ?}}} \cdot \Big\| \underbrace{\mathbf{P}(\mathbf{x}_i,\mathbf{R}_j,\mathbf{t}_j)}_{\substack{\text{predicted}\\ \text{image location}}} - \underbrace{\begin{bmatrix} u_{i,j} \\ v_{i,j} \end{bmatrix}}_{\substack{\text{observed}\\ \text{image location}}} \Big\|^2 \quad (1)$$

The function g is called bundle adjustment and can be solved with algorithms such as that of Levenberg-Marquart.

Features in each photo are detected through feature-detection algorithms (Scale Invariant Feature Transform - SIFT [8], Speeded-Up Robust Features - SURF [9]).

The principle of underwater photogrammetry does not differ from those of terrestrial or aerial photogrammetry, but certain elements that may cause disturbance have to be necessarily considered.

In the paper, underwater photogrammetry was taken into account with the aim of analyzing the effects of different parameters on 3D reconstruction accuracy, such as texturization, water turbidity and ambient light.

II. Materials and Methods

The test geometry chosen for this study is a wind turbine blade (Fig. 2).

A common action camera (GoPro 4 camera black edition) and a commercial software Photoscan (©Agisoft) were used for 3D acquisition and reconstruction of the blade.

Fig. 2 Wind turbine blade

Table 1 reports the main characteristics of the used camera.

Tab. 1 – Main characteristics of GoPro Hero 4 camera

Image Sensor	CMOS 1/2.3"
Resolution	12 MP 4000x3000 pixels
Focal Length	Wide FOV - 14mm Medium FOV - 21mm Narrow FOV - 28mm
Zoom	1x
Opening Maximum	F2.8 fixed focal - wide angle lens 170°
Operating Environment	-40 m
Dimension	41x59x21/30 mm
Weight	88-152g

Photoscan software is based on the Structure for Motion (SfM) approach and bundle adjustment.

The acquisitions were performed in an above ground pool using an equipment properly realized to fix the camera (Fig. 3)

Fig. 3 - Above Ground pool and equipment used to fix the camera

A. *Parameters and conditions set*

All parameters and conditions set for the experimental tests are listed in Table 2 and described below.

Underwater imaging is influenced by the turbidity of the medium, which decreases image contrast and attenuates light intensity. In order to worsen the transparency of water (turbidity) and create a scattering media, different quantities of clay have been suspended in the pool (4x0,85x2 m3). As shown in Table 2, 8 mg/l of clay was released in acquisitions with turbidity set at level 1 (Yes) whereas no clay was released in acquisitions with turbidity set at level 0 (No). The quantity of 8 mg/l has been properly chosen due to the fact that

predesign tests [10] showed that no useful photos would be obtained with larger amounts of clay.

Tab. 2 – List of conditions and parameter sets

Parameters	Levels		
	-1	0	1
Texturization (Tx)	None	Matting only	Yes
Turbidity (T)		None (clear water)	Yes (8mg/l of clay)
Ambient light (Exposure (E))	Night (1/60)	Afternoon (1/30)	Morning (1/15)

In order to study the influence of lightning conditions on underwater photogrammetry, additional parameters have been introduced. In particular, the turbine blade has been studied through three different conditions: clean, matted and textured blade (Fig. 4); and in different phases of the day: morning, afternoon and night.

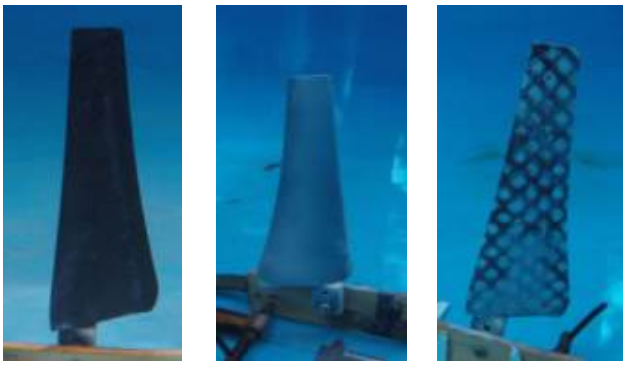

Fig. 4 Turbine blade in three considered conditions: clean, matted, textured

A DoE study with the full factorial experimental plan of 12 acquisitions was carried out (Table 3).

Tab. 3 – Experimental plan of the acquisition tests

Acquisition	Texturization (Tx)	Ambient light	Turbidity (T)	RMSE
1	-1	-1	0	2.727
2	-1	0	0	2.141
3	-1	1	0	1.853
4	0	-1	0	0.996
5	0	0	0	0.968
6	0	1	0	0.863
7	1	-1	0	1.169
8	1	0	0	0.698
9	1	1	0	0.673
10	-1	-1	1	1.911
11	1	0	1	1.822
12	1	1	1	1.866
13	-1	0	1	(∞)
14	-1	1	1	(∞)
15	0	-1	1	(∞)
16	0	0	1	(∞)
17	0	1	1	(∞)
18	1	-1	1	(∞)

B. Experimental tests

A series of measurements was performed inside an above ground pool at the University of Naples, Department of Industrial Engineering.

The pool-based trial was designed to determine about 80 photos for each test. All acquisitions have been made at a distance range of about 500 mm from the subject.

The 3D reconstruction process of the wind turbine blade by Photoscan software (Fig. 5) can be divided in two phases. The first phase consists on the alignment of the acquired images. The position of the image feature points and of the camera, in a local reference system, are detected by means of the SfM algorithm. Starting from the aligned dataset, the second phase consists on the pixel-based reconstruction.

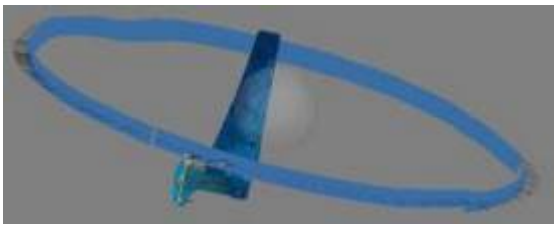

Fig. 5 - 3D reconstruction process of the wind turbine blade by Photoscan software

C. Reference CAD model and comparison

From the acquisitions in the different test conditions, 12 (out of the planned 18) reconstructions were correctly obtained (the first 12 acquisitions reported in Table 3). The last 6 reconstructions suffer from specific combination of condition and parameter set. The 3D reconstructions obtained were then compared with the reference CAD model obtained by means of a high resolution Laser Scanner, VI-9i by Konica Minolta (Fig. 6). In particular, the deviation di (i.e. the shortest distance from the i-th point of the cloud to the CAD nominal model) are recorded over n point of the cloud. Then, the accuracy of the 3D reconstruction is defined as the Root Mean Square Error (RMSE):

$$RMSE = \sqrt{\frac{1}{n}\sum_{i=1}^{n} d_i^2} \qquad (2)$$

over the n points. The accuracy of this non-contact Reverse Engineering system is ±50μm. Data processing was performed in Geomagic Studio software, using an iterative closest point algorithm [11, 12] to minimize the distance between the cloud points and the nominal CAD model.

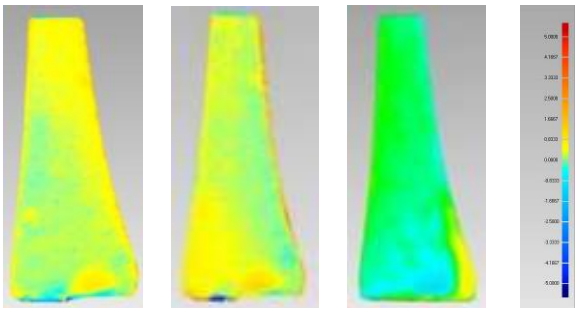

Fig. 6 – Comparison between some of the 3D reconstructions and the reference model

The choice of alignment between point cloud and nominal CAD model should be a noise factor. In this exploration study, it has been considered as a held-constant factor because all parts were aligned using the same procedure and the point clouds were validated by the same expert operator.

III. Analysis of 3D reconstruction via designed experiments for regression

As is known, when missing or faulty data acquisition occur [13] in a design experiment [14], regression methods are extremely useful to correct and still perform adequate analysis. Moreover, many properties of the regression model depend on the levels of the predictor variables. Consequently, in the experimental tests performed in this paper to study 3D reconstruction accuracy (equation (2)), where the levels can be adequately selected, the problem of the Design of Experiments (DoE) [15] naturally arises. The DoE effort in data collection is summarized in Table 3. It resulted very useful to assess the significance of the factors reported in Table 2 even with relatively few acquisitions. However, the influence of the ambient light has not been modeled by the categorical variable reported in Table 3 but through the quantitative parameter exposure (E) which is automatically set by the internal light meter of the GoPro camera. Note that the ISO sensitivity was held constant (100) as well as the aperture (f/2.8) parameter of the camera. The following multiple regression equation with 2 categorical variables Tx and T (Table 3) and the quantitative variable E estimated from the DoE-based acquisitions is reported in Table 4.

Tab. 4 – Multiple regression equations for accuracy of 3D reconstruction (RMSE)

Tx	T	Regression Equation
-1	0	$RMSE = 0.577 + 7.97\ E$
-1	1	$RMSE = \begin{cases} 1.546 + 7.97\ E & \text{if } E < 1/30 \\ \infty & \text{elsewhere} \end{cases}$
0	0	$RMSE = 1.930 + 7.97\ E$
0	1	$RMSE = \infty$
1	0	$RMSE = 0.592 + 7.97\ E$
1	1	$RMSE = \begin{cases} 1.562 + 7.97\ E & \text{if } E > 1/60 \\ \infty & \text{elsewhere} \end{cases}$

The corresponding ANalisys Of VAriance (ANOVA) is reported in Table 5. For each term, the P-Value related to the F-test is smaller than 0.05 and confirms the significance of the factors technologically selected (Table 2) for the quality assessment of the 3D reconstruction.

Tab. 5 – ANOVA table for accuracy of 3D reconstruction (RMSE)

Term	DF	Adj SS	Adj MS	F-Value	P-Value
E	1	0.3067	0.30674	8.36	0.023
Tx	2	3.6236	1.81178	49.38	0.000
T	1	1.8295	1.82947	49.86	0.000
Error	7	0.2568	0.03669		
Total	11	4.8194			

IV. Model adequacy checking

The adequacy of the statistical assumptions is tested through the Normal Probability plot (Fig. 7) and the Residual plot (Fig. 8) performed once having estimated the model. In particular, such plots are reported in order to detect anomalous acquisitions and to check that the errors are uncorrelated and normal distributed with the same variance. Fig. 7 shows an acceptable deviation from the straight line [15] of the normal probability plot of the residuals and therefore, it is likely that the errors are normally distributed with no outliers. In Fig. 8, the plot of the residuals against the fitted values shows that the residuals can be contained in a horizontal band and therefore, there are no obvious model inadequacies. The residuals are plotted versus the fitted values and not versus the actual RMSE values, because they are usually correlated with the latter.

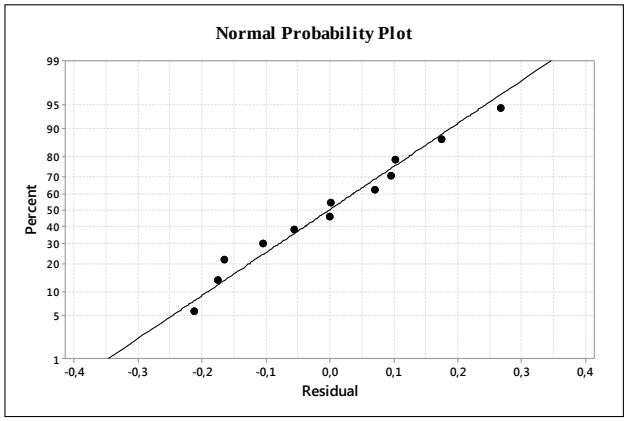

Fig. 7 – Normal probability Plot of Residuals

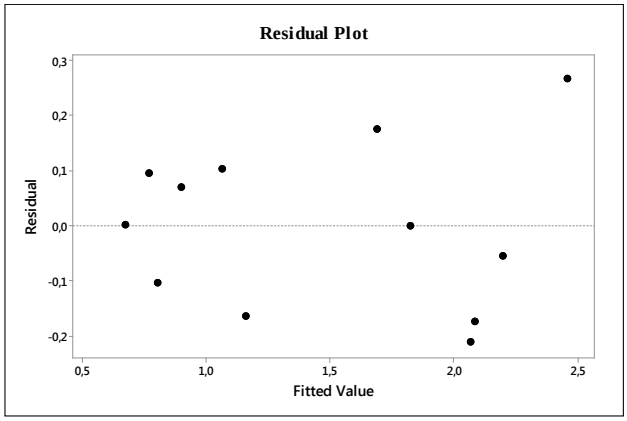

Fig. 8 – Residual Plot (versus Fitted values)

Finally, the main effect plot reported in Fig. 9 can be correctly utilized to characterize the optimal settings of the considered parameters for 3D reconstruction in Underwater Photogrammetry.

Fig. 9 shows that both kinds of texturization are advantageous as well as a morning ambient light. Otherwise, even a moderate quantity of clay (8 mg/l) suspended in the water worsens the reconstruction.

A. *Bootstrap confidence intervals of regression coefficients*

The equation estimated in Table 4 for the accuracy of 3D reconstructions through RMSE, defined in equation (2) are obtained via the least-squares method. Such equations can be also expressed in terms of regression coefficients (RCs) as reported in Table 5.

In order to give a measure of the uncertainties involved in the such estimation [16] method, standard errors (SEs) and confidence intervals (CIs) of RCs are needed. However, standard techniques to estimate SEs and CIs are usually based on large-sample or asymptotic theory. In other words, there is no standard procedure available when data are few as in our case.

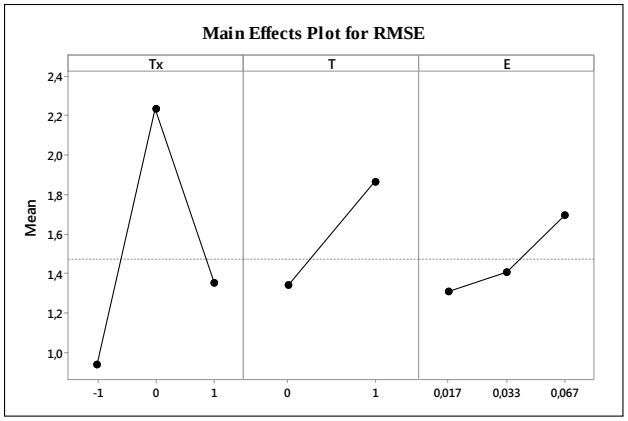

Fig. 9 – Main Effect Plot for RMSE

In these situations, reliable estimates of SEs and CIs can be obtained by bootstrapping [17], which is a computer-intensive approach originally developed by [18].

In particular, the bootstrap sampling procedure, which is utilized in this paper, resamples with replacement from the original data reported in Table 2, n=12 times, yielding a bootstrap sample. Then the regression equation is fitted to this bootstrap sample, resulting in the first least-squares bootstrap estimate of the RCs. This bootstrap sampling procedure has been then repeated m=1000 times.

For each RC, the 5th and the 95th percentiles of the vector of m=1000 bootstrap estimates can be then utilized to calculate the Upper (UBCLs) and Lower (LBCLs) Bootstrap 95%-Confidence Limits. Similarly, for each RC, the corresponding sample standard regression represents the Bootstrap Standard Errors (BSE) reported in Table 6.

B. *Multicollinearity analysis*

In Table 6, the Variance Inflaction Factors (VIFs) [19] are also reported for each term of the regression. VIF is a measure of correlation among parameters (multicollinearity) which may unreasonably inflate the SE of each regression coefficient. In Table 6, VIF values always smaller than 10 indicate that in this case multicollinearity is not influencing regression results and none of the selected parameters (i.e., regressors) should be removed from the model.

A. *Further experiments and confirmation tests*

Let us note from the experimental plan reported in Table3 that the acquisitions 13÷18 did not allow any 3D reconstruction of the blade turbine (Fig.10).

Tab. 6 –Bootstrap Standard errors (BSEs), Upper (UBCLs), Lower (LBCL) 95%-Confidence Limits and Variance Inflaction Factors (VIFs) for regression coefficient estimates (RCs)

Term	RC	SE	LBCL	UBCL	VIF
Constant	1.518	0.126	1,248	1,845	
E	7.97	2.59	1,76	14,01	1.00
Tx					
-1	-0.456	0.0879	-0,6088	-0,1929	1.83
0	0.897	0.0903	0,6893	1,1052	1.83
T					
0	-0.510	0.0686	-0,6900	-0,3298	1.50

Fig. 10 – Wind turbine blade

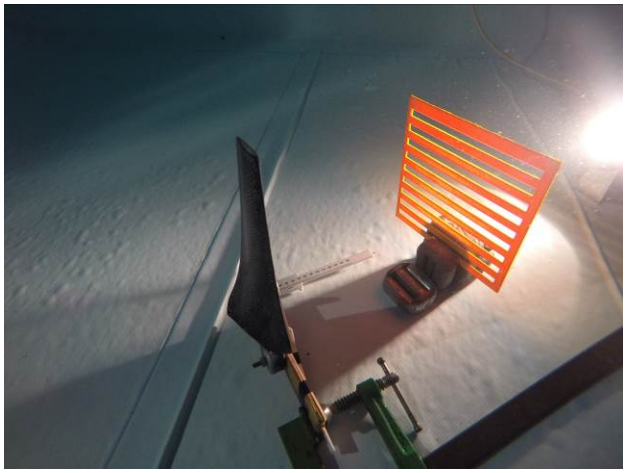

Fig. 11 – Underwater lamp and grids utilized to help reconstruction

However, poor conditions (e.g., very low ambient light and no blade texturization) are the real submarine environment where object texturization is usually unfeasible. In such situations, an additional source of light, e.g., obtained through an underwater

lamp, and one or more grids, which allow a pattern to be created on the edges of the wind turbine blade, may help reconstructionsTherefore, a further experiment is collected in a swimming pool 2 meter deep (Fig 12), with no natural lights nor blade texturization by means of the underwater lamp and grid shown in Fig. 11.

The achieved RMSE is equal to 0.926. In such experimental situation the use of an additional lamp with no grid (to eliminate noise shadows) has proven not to be so advantageous (RMSE=0.7463).

Then, a confirmation test has been has made with a different waterproof camera: the Nikon diploid aw130. Results of the test, for this particular case, confirms the validity of the results obtained by means of the underwater lamp and grid (RMSE=1.513).

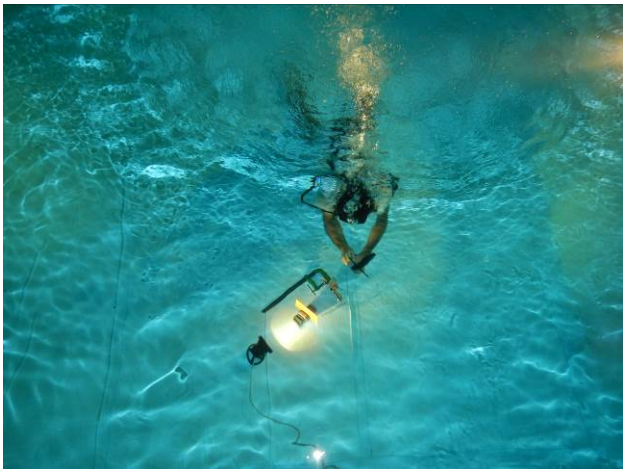

Fig. 12 – Experimental environment

These results are then comparable with those obtained with natural ambient light (Table 3). In order to apply the subject of this paper to real conditions, a sea trial was finally performed.

The comparison between the 3D model obtained by the acquisition in sea, on the matting blade and reference model, shows a standard deviation of 0.64 mm and a RMS error of 0.90 mm (Fig. 13).

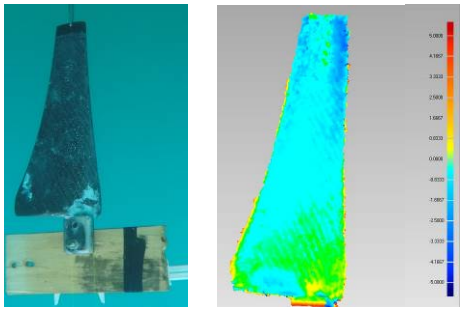

Fig. 13– Sea trial: comparison between the obtained 3D model (matting blade) and reference model

V. Conclusion

The paper presents an experimental study on the underwater photogrammetry. A photogrammetric approach based on Structure for Motion algorithms and successive bundle adjustment is applied for the 3D reconstructions of a wind turbine blade. Different conditions were performed and analyzed through designed experiments for regression in order to reduce acquisitions needed to achieve reliable conclusions. Photos were acquired in an above ground pool. With respect to the quality of the 3D reconstruction, the results show that blade texturization, ambient light and water turbidity are significant parameters.

In particular, the blade texturization significantly helps the quality of the 3D reconstruction and the optimal results are obtained with the higher level of the ambient light (exposure 1/60, f/2.8 and ISO sensitivity 100) and clear water. Some parameter combinations (e.g., turbid water, clean blade) do not allow any 3D reconstruction.

However, further tests conducted by means of a waterproof lamp and a grid, which allows a pattern to be created on the edges of the wind turbine blade, are found suitable in poor experimental conditions (e.g., in real submarine environment) and comparable with those obtained with natural ambient light.

Acknowledgement

The authors gratefully acknowledge the Engineers Luca Buonissimo, Pasquale Purcaro, Gabriele Martignetti and Gabriele Staiano for their useful technical support. They are also deeply grateful to Engineer Roberto Correro for having directed of the experimental environment.

References

[1] Martínez S., Cuesta E., Barreiro J., Álvarez B., Analysis of laser scanning and strategies for dimensional and geometrical control, Int J Adv Manuf Technol, 46: 621–629, 2010.

[2] Martorelli M., Pensa C., Speranza D., Digital Photogrammetry for Documentation of Maritime Heritage, Journal of Maritime Archaeology, 9(1), pp. 81-93, 2014.

[3] Fonstad, M. A., Dietrich, J., T., Courville, B. C., Jensen, J. L., Carbonneau P. E., Topographic structure from motion: a new development in photogrammetric measurement. Eart. Surf. Process. Landforms, 38, pp. 421-430, 2013.

[4] Green, S., Bevan A., Shapland, M., A comparative assessment of structure from motion methods for archaeological research, Journal of Archaeological Science, 46, pp. 173-181, 2014.

[5] Burtch R., History of Photogrammetry. Technical report, The Center for Photogrammetric Training, Ferris State University, pp. 1-36, 2008.

[6] Triggs B., McLauchlan P., Hartley R., Fitzgibbon A., Bundle Adjustment — A Modern Synthesis". ICCV '99: Proceedings of the International Workshop on Vision Algorithms, Springer-Verlag, pp. 298–372, 1999.

[7] Ullman S., The interpretation of structure from motion. Proc. R. Soc. Lond. B, 203, pp. 405–426, 1979.

[8] Lowe D. G., Distinctive Image Features from Scale-Invariant Keypoints, International Journal of Computer Vision, vol. 60 (2), pp. 91-110, 2004.

[9] Bay H., Ess T., Tuytelaars, Vasn Gool L., SURF: Speeded Up Robust Features, Computer Vision and Image Understanding (CVIU), vol. 110 (3), pp. 346-359, 2008.

[10] Bianco G., Gallo A., Bruno F., Muzzupappa M., A comparative analysis between active and passive techniques for underwater 3D reconstruction of close-range objects, Sensors, Vol. 13, n. 8, pp. 11007-11031, 2013.

[11] Besl P. J., McKay N. D., A Method for Registration of 3-D Shapes, IEEE Trans. Pattern Anal. Mach. Intell., 14(2), pp. 239–256, 1992.

[12] Pottmann H., Leopoldseder S., Hofer M., Simultaneous Registration of Multiple Views of a 3D Object, Proceedings PCV'02, Archives of the Photogrammetry, Remote Sensing and Spatial Information Sciences,

Vol. XXXIV, Part 3A, Commission III, Graz, Australia, Sept. 9–13, pp. 265–270, 2002.
[13] López-Molina, Thomás, Anna Pérez-Méndez, and Francklin Rivas-Echeverría. "Missing values imputation techniques for neural networks patterns." WSEAS International Conference. Proceedings. Mathematics and Computers in Science and Engineering. Eds. N. E. Mastorakis, et al. No. 12. WSEAS, 2008.
[14] Roozen-Kroon, P. J. M., A. J. G. Schoofs, and D. H. Van Campen. "Fast numerical shape optimization of bells using design of experiment and regression techniques." Computer aided Optimum Design of Structures, Computational Mechanics Publications. Heidelberg: Springer Verlag (1989).
[15] Daniel C., Wood F. Fitting Equation to Data, 2nd ed. Wiley & Sons, 1980.
[16] Coleman H., Steele W., Experimentation and Uncertainty Analysis for Engineers, Wiley & Sons, 1989.
[17] Norazan, M. R., M. Habshah, and A. H. M. R. Imon. "Weighted Bootstrap with Probability in Regression." WSEAS International Conference. Proceedings. Mathematics and Computers in Science and Engineering. Ed. Shengyong Chen. No. 8. World Scientific and Engineering Academy and Society, 2009.
[18] Efron, Bradley, and B. Efron. The jackknife, the bootstrap and other resampling plans. Vol. 38. Philadelphia: Society for industrial and applied mathematics, 1982.
[19] Marquardt D., Generalized inverses, ridge regression, biased linear estimation, and nonlinear estimation, Technometrics 12, pp. 591-612, 1970.